Nonretarded limit of the Lifshitz theory for a wedge

R. Krechetnikov and A. Zelnikov [*]

Departments of Mathematical & Statistical Sciences, and Physics, University of Alberta, Edmonton, Alberta, Canada T6G 2E1

(Received 1 April 2021; revised 21 November 2021; accepted 18 January 2022; published 7 February 2022)

We develop the nonretarded limit of the Lifshitz theory of van der Waals forces in a wedge of a dielectric material. The nonplanar geometry of the problem requires determining the pointwise distribution of stresses. The findings are relevant to a wide range of phenomena from crack propagation to contact-line motion. First, the stresses prove to be anisotropic as opposed to the classical fluid-mechanics treatment of the contact-line problem. Second, the wedge configuration is always unstable, with its angle tending either to collapse or to unfold. The presented theory unequivocally demonstrates the quantum nature of the forces dictating the wedge behavior, which cannot be accounted for with classical methods.

DOI: 10.1103/PhysRevA.105.022802

I. INTRODUCTION

Pressure in microscopically thin films is generally different from that in the macroscopic bulk due to the action of van der Waals forces [1,2] leading to disjoining pressure Π_D. Originally, it was calculated for pure substances [3], under the assumption of additivity, via pairwise summation of the attractive nonretarded part of the intermolecular potential $\varphi_{\rm vdW} \sim r^{-6}$:

$$\Pi_D(\ell) = -A_H/6\pi\ell^3, \quad (1.1)$$

where ℓ the film thickness and A_H the Hamaker constant [4] specific to a given combination of substances in contact. Motivated by the discrepancy [5] between experiments [6] and the "additive" calculations, Lifshitz [7] rigorously derived Π_D for dispersion forces [8] with quantum field theory methods, thus recognizing their genuine quantum nature and nonadditivity [9,10], and naturally expressed A_H in terms of imaginary parts of the substances dielectric constants, in accordance with the fluctuation-dissipation theorem [11,12]. This dispersive part of van der Waals forces is always present as a consequence of quantum fluctuations in the dielectric molecules' polarizability and plays a key role in a host of everyday phenomena such as adhesion, surface tension, adsorption, wetting, and crack propagation in solids, to name a few [13]. Since Π_D is generally prevalent at $\ell \lesssim 1\,\mu$m, it controls the stability and wettability of liquid films. Because of the constant value of this stress $\Pi_D(\ell) \equiv -\sigma_{zz}$ across the film, it simply provides a jump in the total hydrodynamic pressure [see Fig. 1(a)]. However, per (1.1) Π_D formally diverges as $\ell \to 0$ and hence appears to be invalid in modeling liquid films terminating at the substrate, which, in repetition of the history behind (1.1), has led to a number of attempts [14] along the lines of the "additive" macroscopic theory [3] to generalize and regularize $\Pi_D(\ell)$ for the wedge configuration [see Fig. 1(b)]. They not only ignored the nonadditive nature of dispersion forces, which becomes especially important in view of the nonplanar geometry of the problem thus affecting the stress distribution, but also relied upon the unjustified assumption of an isotropic pressure across the wedge, in which anisotropy in the stress tensor near the interface is expected [15,16]. Moreover, *a priori* it is clear that the formal singularity when $\ell \to 0$ cannot be resolved in the framework of van der Waals force calculations without proper analysis of UV divergences. It is natural to expect, nevertheless, that the characteristic UV cutoff should be on the order of intermolecular separation a_0, at which long-range attraction forces are counterbalanced by the short-range repulsive ones. Therefore, to properly account for van der Waals stresses in a wedge, one must generalize the Lifshitz planar film theory in order to determine local behavior of the stresses and, in particular, to understand the stability of the wedge configuration considered here in thermal equilibrium.

Previously, using Schwinger's source theory [17], a rigorous calculation of stresses in the Casimir (retarded) limit was performed in the vacuum wedge region bounded by perfectly conducting walls [18,19]; the dispersion forces in this case are due to retarded potentials $\varphi_{\rm vdW} \sim r^{-7}$ only. The same problem was generalized to the case when the wedge is filled with an isotropic and nondispersive medium [20] and with two dielectric media separated by an arc of a perfectly conducting cylindrical shell [21,22]. Here, however, we are interested in dispersion forces in dielectrics and on shorter distances ℓ where retarded effects are no longer important, i.e., distances smaller than the wavelength λ_a of the electromagnetic (EM) absorption peak but larger than a_0. At these scales the leading contribution to the stresses comes only from fluctuations of the electric field, which in the Coulomb gauge is given by a gradient of the time-dependent potential A_0. The fluctuating spatial components of the vector potential A_i are responsible for retardation effects. They are important for the computation of the Casimir effect at scales larger than λ_a, e.g., for water $\lambda_a = O(10^3)$ nm, but are negligible compared to the nonretarded contributions at smaller scales.

[*]zelnikov@ualberta.ca

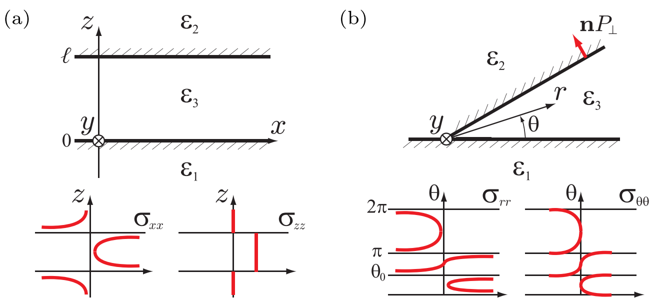

FIG. 1. Two basic configurations: (a) slit and (b) wedge.

II. NONRETARDED GREEN'S FUNCTION

In the equilibrium case, when there are no fluxes, the EM stress-energy tensor $T^{\mu\nu} = F^{\mu\alpha} D^{\nu}{}_{\alpha} - \frac{1}{4} g^{\mu\nu} F_{\alpha\beta} D^{\alpha\beta}$ [23], where $F^{\mu\nu}$ and $D^{\mu\nu}$ are the Maxwell field and displacement tensors, respectively, and $g^{\mu\nu}$ is the Minkowski metric with the signature $(-+++)$, takes the form $T^{\mu\nu} = \mathrm{diag}(\varrho, -\sigma^{ij})$; here $i, j = (x, y, z)$, $\mu, \nu = (t, x, y, z)$, $\varrho = T^{00}$ the EM energy density, and σ^{ij} the EM stress tensor with the standard convention on its signs [24]. In what follows, we will adopt Planck units, in which $\hbar = c = k_B \equiv 1$, and restore SI units whenever computations are performed. Since we are interested in the nonretarded limit, it proves to be convenient to use the Coulomb gauge $\nabla^i A_i = 0$, which in this limit allows the components of the vector potential to reduce to $A_0 = -\phi$ and $A_i = 0$. Then, the Maxwell equations simplify to a single equation for $A_0(t, \boldsymbol{r})$:

$$\nabla_i(\varepsilon(\boldsymbol{r})\nabla^i)A_0(t, \boldsymbol{r}) = -j_0(t, \boldsymbol{r}), \tag{2.1}$$

where j_0 is the fluctuating charge density. It is important to bear in mind that even though only spatial derivatives enter the operator in this equation, the electric potential is time dependent, and its dynamics is governed by the fluctuating dipole moments of the dielectric medium. Also note that quantum fluctuations of dipoles involve all frequencies. Then, the Feynman propagator $G^F(t, \boldsymbol{r}; t', \boldsymbol{r}') \equiv G^F_{00}(t, \boldsymbol{r}; t', \boldsymbol{r}')$ is the vacuum expectation value (ground states corresponding to zero temperature) of the product of field operators $i\langle \mathrm{T}\mathrm{A}_0(t, \boldsymbol{r})\mathrm{A}_0(t', \boldsymbol{r}')\rangle$; here A_0 stands for operators, the brackets $\langle \cdots \rangle$ denote averaging with respect to the ground state of the system, and the symbol T is the chronological product, i.e., the operators following it should be arranged from right to left in order of increasing time. $G^F(t, \boldsymbol{r}; t', \boldsymbol{r}')$ obeys

$$\nabla_i(\varepsilon(\boldsymbol{r})\nabla^i)\, G^F(t, \boldsymbol{r}; t', \boldsymbol{r}') = \delta(t, t')\delta(\boldsymbol{r}, \boldsymbol{r}'); \tag{2.2}$$

here $\delta(\boldsymbol{r}, \boldsymbol{r}') = \delta(\boldsymbol{r} - \boldsymbol{r}')/\sqrt{-g}$, and $\sqrt{-g} = r$ in the cylindrical system of coordinates $\boldsymbol{r} = (y, r, \theta)$ [see Fig. 1(b)].

When fluctuations are predominantly quantum [25] at the absorption frequency ω_a, e.g., for water $T \leqslant \omega_a = O(10^3)$ K, the Green's function of a macroscopic system (like ours) at nonzero temperatures differs from that at zero temperature only in that the averaging with respect to the ground state of a closed system is replaced by averaging over the Gibbs distribution, namely ensemble averages with thermal states at temperature $T \equiv \beta^{-1}$. The thermal Green's function $G^\beta(t, \boldsymbol{r}; t', \boldsymbol{r}')$ can be obtained from the Feynman one using the Wick rotation: substitution of $t = -it_E$ in the Lorentzian Green's function to produce Euclidean one $G^\beta(t_E, \boldsymbol{r}, \boldsymbol{r}') = i\, G^F(it_E, \boldsymbol{r}, \boldsymbol{r}')$, which is periodic in Euclidean time t_E with period β; we also took into account the homogeneity of the Green's function in time and inhomogeneity in space in view of the presence of boundaries. Due to periodicity in Euclidean time, one can decompose $G^\beta(t_E, \boldsymbol{r}, \boldsymbol{r}')$ and other related Green's functions in the Fourier time series:

$$G^\beta(t_E, \boldsymbol{r}, \boldsymbol{r}') = \frac{1}{\beta}\sum_{n=-\infty}^{\infty} \widehat{G}^\beta(\zeta_n; \boldsymbol{r}, \boldsymbol{r}')\, e^{i\zeta_n t_E}; \tag{2.3}$$

here $\zeta_n = 2\pi n/\beta$ are the Matsubara frequencies, and $\widehat{G}^\beta(\zeta_n; \boldsymbol{r}, \boldsymbol{r}')$ the solution of the Fourier transformed equation (2.2), which in cylindrical coordinates reads

$$\nabla_i(\varepsilon(\zeta_n)\nabla^i)\widehat{G}^\beta(\zeta_n; \boldsymbol{r}, \boldsymbol{r}') = \frac{\delta(r - r')\delta(\theta - \theta')\delta(y - y')}{r}. \tag{2.4}$$

At the interface Σ between media a and b with the corresponding dielectric constants ε_a and ε_b one has to satisfy the usual boundary conditions for the electric field [26],

$$\widehat{G}^\beta_a\big|_{\boldsymbol{r}\in\Sigma} = \widehat{G}^\beta_b\big|_{\boldsymbol{r}\in\Sigma}, \tag{2.5a}$$

$$\varepsilon_a n^i \nabla_i\, \widehat{G}^\beta_a\big|_{\boldsymbol{r}\in\Sigma} = \varepsilon_b n^i \nabla_i\, \widehat{G}^\beta_b\big|_{\boldsymbol{r}\in\Sigma}, \tag{2.5b}$$

where n^i is the normal vector to Σ. The constructed Green's function $\widehat{G}^\beta(\zeta_n; \boldsymbol{r}, \boldsymbol{r}')$ also must be periodic in θ with period 2π as per the problem statement [see Fig. 1(b)].

Applying the Fourier transform in the y direction and, since EM surface waves decay exponentially away from the interface [7], the Kontorovich-Lebedev transform [22,27,28] in the radial r direction to a function $f(r, y)$ furnishes

$$\widetilde{f}(\nu, k) = \int_{-\infty}^{\infty} e^{-iky}\, dk \int_0^\infty dr\, f(r, y)\, K_{i\nu}(kr)\, r^{-1}, \tag{2.6}$$

where k is the momentum conjugate to the coordinate y along the edge, ν has the meaning of a momentum conjugate to the radial coordinate r, and $K_{i\nu}(kr)$ are the modified Bessel functions of the second kind. After rescaling the Green's function, transformed according to (2.6), $\widetilde{G}^\beta \to \Phi_\nu e^{-iky'} K_{i\nu}(kr')$, we arrive at the boundary-value problem for the angular function $\Phi_\nu(\theta, \theta')$:

$$\begin{gathered}
\left(\frac{\partial^2}{\partial\theta^2} - \nu^2\right)\Phi_\nu(\theta, \theta') = \frac{1}{\varepsilon}\,\delta(\theta - \theta'),\\
\Phi_\nu|_{\theta=\theta_0+0} = \Phi_\nu|_{\theta=\theta_0-0}, \quad \varepsilon_2\partial_\theta\Phi_\nu|_{\theta=\theta_0+0} = \varepsilon_3\partial_\theta\Phi_\nu|_{\theta=\theta_0-0},\\
\Phi_\nu|_{\theta=\pi+0} = \Phi_\nu|_{\theta=\pi-0}, \quad \varepsilon_1\partial_\theta\Phi_\nu|_{\theta=\pi+0} = \varepsilon_2\partial_\theta\Phi_\nu|_{\theta=\pi-0},\\
\Phi_\nu|_{\theta=+0} = \Phi_\nu|_{\theta=2\pi-0}, \quad \varepsilon_3\partial_\theta\Phi_\nu|_{\theta=+0} = \varepsilon_1\partial_\theta\Phi_\nu|_{\theta=2\pi-0}.
\end{gathered} \tag{2.7}$$

For $0 \leqslant \theta' \leqslant \theta_0$, the solution takes the form

$$\Phi_\nu(\theta,\theta') = \begin{cases} ve^{-\nu\theta} + de^{-2\pi\nu}e^{\nu\theta}, & \pi < \theta < 2\pi, \\ ae^{-\nu\theta} + ue^{\nu\theta}, & \theta_0 < \theta < \pi, \\ be^{\nu\theta} + ce^{-\nu\theta} - \frac{1}{2\nu\varepsilon_3}e^{-\nu|\theta-\theta'|}, & 0 < \theta < \theta_0, \end{cases}$$

where the unknown constants are determined by the boundary conditions in (2.7). The inverse transform corresponding to (2.6) is given by

$$\widehat{G}^\beta(\zeta_n;\boldsymbol{r},\boldsymbol{r}') = \frac{1}{\pi^3}\int_{-\infty}^{\infty} e^{ik(y-y')}\,dk \int_0^\infty \nu\,\sinh(\pi\nu)\,d\nu \times \Phi_\nu(\theta,\theta')\,K_{i\nu}(kr)\,K_{i\nu}(kr'). \tag{2.8}$$

In the homogeneous case, when the entire space has the dielectric permittivity equal to that in the wedge $\varepsilon_1 = \varepsilon_2 \equiv \varepsilon_3$, solving (2.7) leads to

$$\Phi^0_\nu(\theta,\theta') = -\frac{1}{2\nu}\left[e^{-\nu|\theta-\theta'|} + \frac{2\cosh[\nu(\theta-\theta')]}{e^{2\pi\nu}-1}\right]. \tag{2.9}$$

For calculations of the renormalized stress tensor at $\theta = \theta'$ we need to know only the renormalized function

$$\Delta\Phi_\nu(\theta,\theta') = \Phi_\nu(\theta,\theta') - \Phi^0_\nu(\theta,\theta'). \tag{2.10}$$

For $0 < \theta, \theta' < \theta_0$,

$$\Delta\Phi_\nu(\theta,\theta') = -\frac{1}{2\nu}\left[\frac{Z}{W} - \frac{2\cosh[\nu(\theta-\theta')]}{e^{2\pi\nu}-1}\right], \tag{2.11}$$

where

$$W = \lambda_{+++}\cosh 2\pi\nu - \lambda_{+--}\cosh 2\nu(\pi-\theta_0) + \lambda_{-+-}\cosh 2\nu\theta_0 - (\lambda_{--+} + \lambda_0), \tag{2.12a}$$

$$Z = \lambda_{---}\sinh\nu[\theta+\theta'-2\theta_0] + \lambda_{+-+}\sinh\nu[\theta+\theta'-2\pi] - \lambda_{-++}\sinh\nu[\theta+\theta'] - \lambda_{++-}\sinh\nu[\theta+\theta'+2(\pi-\theta_0)] + [\lambda_{+--}e^{\nu(2\pi-\theta_0)} - \lambda_{-+-}e^{-2\nu\theta_0} + (\lambda_{--+}+\lambda_0) - \lambda_{+++}e^{-2\pi\nu}]\cosh\nu[\theta-\theta']; \tag{2.12b}$$

above we introduced the notations $\lambda_0 = 8\,\varepsilon_1\varepsilon_2\varepsilon_3$ and $\lambda_{\pm\pm\pm} = (\varepsilon_1 \pm \varepsilon_2)(\varepsilon_1 \pm \varepsilon_3)(\varepsilon_2 \pm \varepsilon_3)$. Note that the solution for $\theta \in (\theta_0, \pi)$ can be found from (2.11) with the substitution $\varepsilon_1 \to \varepsilon_1$, $\varepsilon_2 \to \varepsilon_3$, $\varepsilon_3 \to \varepsilon_2$, $\theta_0 \to \pi - \theta_0$, $\theta \to \pi - \theta$, and the ensuing replacements in λ's.

III. STRESSES IN THE WEDGE

A. General expressions

With the determined Green's function (2.8), we are in a position to calculate the stress tensor (see Appendix B):

$$\sigma_{ij}(t_E,\boldsymbol{r},\boldsymbol{r}') = -\varepsilon\left[A_{t_E;i}A_{t_E;j} - \tfrac{1}{2}g_{ij}\,A_{t_E;k}A_{t_E;k}\right], \tag{3.1}$$

where the components are written in the coordinate basis and the semicolon implies the covariant derivative; the covariant form is chosen for convenience because we work in the non-Cartesian coordinates. The spatial components g^{ij} of the metric tensor in cylindrical coordinates are $g_{ij} = g^{ij} = 0$ for $i \neq j$, $g^{yy} = 1$, $g^{rr} = 1$, and $g^{\theta\theta} = r^{-2}$. The Fourier transform $\widehat{\sigma}_{ij'}(\zeta_n;\boldsymbol{r},\boldsymbol{r}')$ of the stress tensor $\sigma_{ij'}(t_E,\boldsymbol{r},\boldsymbol{r}')$ is defined similar to (2.3). The renormalized Fourier components of the stress tensor $\Delta\sigma_{ij'}(\zeta_n;\boldsymbol{r},\boldsymbol{r}') = \widehat{\sigma}_{ij'}(\zeta_n;\boldsymbol{r},\boldsymbol{r}') - \widehat{\sigma}^{(\mathrm{div})}_{ij'}(\zeta_n;\boldsymbol{r},\boldsymbol{r}')$, which for brevity we denote by $\overline{\sigma}_{ij'}(\zeta_n;\boldsymbol{r},\boldsymbol{r}')$, can be written in terms of the renormalized Fourier components $\Delta\widehat{G}^\beta_{;ij'} = \widehat{G}^\beta_{;ij'} - \widehat{G}^{\beta(\mathrm{div})}_{;ij'}$ of the thermal Green's function

$$\overline{\sigma}_{ij'}(\zeta_n;\boldsymbol{r},\boldsymbol{r}') = -\varepsilon_3\left[\Delta\widehat{G}^\beta_{;ij'} - \tfrac{1}{2}g_{ij'}\,g^{kk'}\,\Delta\widehat{G}^\beta_{;kk'}\right] \tag{3.2a}$$

$$+ \tfrac{1}{2}g_{ij'}\,\rho\,\tfrac{\partial\varepsilon_3}{\partial\rho}\,g^{kk'}\,\Delta\widehat{G}^\beta_{;kk'}, \tag{3.2b}$$

so that $\overline{\sigma}_{ij} = g_j{}^{j'}\overline{\sigma}_{ij'}$, and then one can take the limit of coincident points $\overline{\sigma}_{ij}(\zeta_n;\boldsymbol{r}) = \overline{\sigma}_{ij}(\zeta_n;\boldsymbol{r},\boldsymbol{r}')|_{\boldsymbol{r}=\boldsymbol{r}'}$. Here $g_{ij'}(\boldsymbol{r},\boldsymbol{r}')$ is the operator of parallel transport, which reduces to the metric $g_{ij'}(\boldsymbol{r},\boldsymbol{r}')|_{\boldsymbol{r}=\boldsymbol{r}'} = g_{ij}(\boldsymbol{r})$. Similar to thin films [29] and according to the general theory [26], in a wedge the isotropic electrostriction part (3.2b) of the stress tensor is absorbed [30], along with the UV-divergent stress $\sigma^{(\mathrm{div})}_{ij}$ originating from the divergent Green's function (2.9), by the bare mechanical stress $\sigma^{(\mathrm{m})}_{ij}$ to produce the isotropic renormalized mechanical pressure $\sigma^{(\mathrm{ren})}_{ij} = -\delta_{ij}p^{(\mathrm{ren})}$ [31]. Therefore, in what follows we omit the electrostriction term (3.2b) since it does not contribute to the renormalized force.

Altogether, the Fourier stress-tensor components at ζ_n are, after raising indices $\overline{\sigma}^{ij} = g^{ik}g^{jl}\overline{\sigma}_{kl}$ to be consistent with the dynamic equations [32],

$$\overline{\sigma}^{\theta\theta} = \frac{1}{r^5}\int_0^\infty d\widetilde{\nu}\left[2\frac{\partial^2\Delta\Phi_\nu}{\partial\theta\partial\theta'} - (1+2\nu^2)\Delta\Phi_\nu\right]_{\theta=\theta'}, \tag{3.3a}$$

$$\overline{\sigma}^{rr} = \frac{1}{r^3}\int_0^\infty d\widetilde{\nu}\left[\frac{1}{2}\Delta\Phi_\nu - 2\frac{\partial^2\Delta\Phi_\nu}{\partial\theta\partial\theta'}\right]_{\theta=\theta'}, \tag{3.3b}$$

$$\overline{\sigma}^{yy} = -\frac{1}{r^3}\int_0^\infty d\widetilde{\nu}\left[\frac{1}{2}\Delta\Phi_\nu + 2\frac{\partial^2\Delta\Phi_\nu}{\partial\theta\partial\theta'}\right]_{\theta=\theta'}, \tag{3.3c}$$

$$\overline{\sigma}^{r\theta} = \overline{\sigma}^{\theta r} = -\frac{1}{r^4}\int_0^\infty d\widetilde{\nu}\;2\left[\frac{\partial\Delta\Phi_\nu}{\partial\theta}\right]_{\theta=\theta'}, \tag{3.3d}$$

where the measure is $d\widetilde{\nu} = \frac{1}{16\pi}d\nu\,\nu\tanh(\pi\nu)$, while $\Delta\Phi_\nu$, $\partial_\theta\Delta\Phi_\nu$, and $\partial_\theta\partial_{\theta'}\Delta\Phi_\nu$ are computed from (2.11). Naturally, in view of symmetries, $\overline{\sigma}^{y\theta}(\zeta_n;\boldsymbol{r}) = 0$ and $\overline{\sigma}^{yr}(\zeta_n;\boldsymbol{r}) = 0$. The integrals over ν in (3.3) converge since all integrands are functions of $\Delta\Phi_\nu$ (2.11), which at every point outside the interfaces fall off exponentially at large ν. The UV-divergent vacuum contribution was taken care of using the Lifshitz procedure $\Phi_\nu(\theta,\theta') \to \Delta\Phi_\nu(\theta,\theta')$ (2.10), which means subtraction of local vacuum contributions to stresses of the media with the same local ε but without boundaries. The appearance of off-diagonal stress components $\overline{\sigma}^{r\theta} = \overline{\sigma}^{\theta r}$ is notable and due to the influence of interfaces meeting at an angle θ_0.

B. Limit to a slit

The limit of a slit [7] [see Fig. 1(a)] can be recovered from (3.3) as it corresponds to the region away from the wedge apex $r \to \infty$ and $\theta_0 \to 0$ while keeping $\ell = r\theta_0 = \text{const}$; for that we denote $\nu = qr = q\ell/\theta_0$, where $q = \sqrt{q_x^2 + q_y^2}$ is the wave number in the (x, y) plane. Then $\frac{1}{r^3}\nu^2 d\nu = q^2 dq$, so that (3.3a) produces in medium 3

$$\overline{\sigma}^{zz} = -\frac{1}{2\pi}\int_0^\infty dq\, q^2 \frac{1}{\frac{\varepsilon_1+\varepsilon_3}{\varepsilon_1-\varepsilon_3}\frac{\varepsilon_2+\varepsilon_3}{\varepsilon_2-\varepsilon_3}e^{2q\ell} - 1}, \tag{3.4}$$

while in medium 2 it vanishes identically, $\overline{\sigma}^{zz}(z) \equiv 0$; this is exactly the nonretarded limit taken from the complete relativistic Lifshitz theory [33] but obtained here via solving the problem in the nonretarded setting from the very beginning. To further convince the reader of the validity of such an approach, in Appendix A we consider in greater detail a building block of the Lifshitz theory: the classical problem of Casimir and Polder [34] of interaction between a time-dependent dipole and a dielectric half-space.

The other stress-tensor component in medium 3 reads

$$\overline{\sigma}^{xx} = -\frac{1}{8\pi}\int_0^\infty dq\, q^2 \frac{2 + \frac{\varepsilon_1+\varepsilon_3}{\varepsilon_1-\varepsilon_3}e^{2qz} + \frac{\varepsilon_2+\varepsilon_3}{\varepsilon_2-\varepsilon_3}e^{2q(\ell-z)}}{\frac{\varepsilon_1+\varepsilon_3}{\varepsilon_1-\varepsilon_3}\frac{\varepsilon_2+\varepsilon_3}{\varepsilon_2-\varepsilon_3}e^{2q\ell} - 1}, \tag{3.5}$$

with $\overline{\sigma}^{yy} = \overline{\sigma}^{xx}$, indicating that near the boundary $z \to \ell$ the local stresses $\overline{\sigma}^{xx}$ and $\overline{\sigma}^{yy}$ diverge [see Fig. 1(a)]; similarly in medium 2

$$\overline{\sigma}^{xx} = \frac{1}{8\pi}\int_0^\infty dq\, q^2 e^{-2q(z-\ell)} \frac{\frac{\varepsilon_1+\varepsilon_3}{\varepsilon_1-\varepsilon_3}e^{2q\ell} - \frac{\varepsilon_2+\varepsilon_3}{\varepsilon_2-\varepsilon_3}}{\frac{\varepsilon_1+\varepsilon_3}{\varepsilon_1-\varepsilon_3}\frac{\varepsilon_2+\varepsilon_3}{\varepsilon_2-\varepsilon_3}e^{2q\ell} - 1}, \tag{3.6}$$

even if it is the vacuum, and the divergence is not removed by renormalization [35]; see also analogous calculations [35–39] showing that the tangential stress $\overline{\sigma}_{xx}$ is divergent. This behavior arises because of the nonphysical nature of the sharp interface boundary condition [39] associated with the jump in ε and the high wave number (momenta) q of the virtual photon behavior in the idealized spectral representation of the stress leading to the divergent integrand $\sim q^2$, while in reality there must be a cutoff [29] at some $q_{\max}$, which is on the order of the reciprocal of the interatomic spacing a_0^{-1} [39]. The equivalence of the latter divergence to that due to the sharp interface condition is easy to see from the corresponding equation for the Fourier components of the Green's function when interface is smeared on the length scale λ:

$$\{\partial_z[\varepsilon(z/\lambda)\,\partial_z] - q^2\}\widetilde{G}^\beta = -\delta(z - z'),\ z \pm \infty:\ \widetilde{G}^\beta \to 0;$$

clearly, the problem in z becomes scale free after the transformation $z \to \kappa\widetilde{z}$, while $q^2 \to \kappa^2 q^2$, thus indicating that the limit to a sharp interface $\kappa \to 0$ is equivalent to the limit $q \to \infty$. The divergences in both stress-tensor components $\overline{\sigma}^{yy}$ and $\overline{\sigma}^{xx}$ are proportional to $\varepsilon_2 - \varepsilon_3$, indicating that the resulting stresses may be seen as stretching (expanding) or shrinking (compressing, such as surface tension) the interface depending upon the media in which the effect is considered. From the conservation law, the energy density $\epsilon(z) = \overline{\sigma}^{xx}(z) + \overline{\sigma}^{yy}(z) + \overline{\sigma}^{zz}(z)$ is divergent as well, which is a known effect near boundaries in the context of local analysis of the Casimir effect [35,36]. The tangential diverging stresses are responsible for the surface-tension phenomena [39].

For a wedge, we note that divergences in stresses (3.3) appear already in the normal to the interface stress component

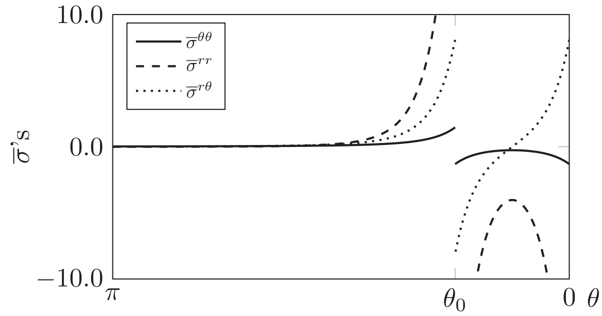

FIG. 2. Plots of stress-tensor components scaled with respect to $16\pi\beta r^n$ with the exponent n adequate for the respective component as per (3.3) at a single absorption frequency and in the case $\theta_0 = \pi/4$, $\varepsilon_1 = \varepsilon_2 = 2$, $\varepsilon_3 = 1$, i.e., corresponding to a crack in a dielectric. Integration is performed up to $\nu_{\max}$.

$\overline{\sigma}^{\theta\theta}$ if integration is performed with respect to ν to infinity. However, in the context of the wedge geometry it is clear that since the interface between media has thickness $\delta\theta \sim 1/(2\nu)$ in the angle coordinate and the shortest distance to be resolved is intermolecular $a_0 \sim \delta\theta\, r$, we find the physically allowed maximum value of ν to be $\nu_{\max} \sim r/(2a_0)$; e.g., for $r \sim 10\, a_0$, $\nu_{\max} = 5$. Typical stress distributions, clearly demonstrating anisotropy, are shown in Fig. 2 for the vacuum wedge surrounded by a sole dielectric material. The case when the dielectric wedge of the same angle is surrounded by the vacuum is a mirror reflection of Fig. 2 with respect to the abscissa.

IV. MECHANICAL EQUILIBRIUM OF THE WEDGE

The next question to consider is on mechanical equilibrium of the wedge. The force density $f^i = \overline{\sigma}^{ik}{}_{;k}$ reads

$$f^\theta = \partial_\theta\overline{\sigma}^{\theta\theta} + \partial_r\overline{\sigma}^{\theta r} + \frac{3}{r}\overline{\sigma}^{\theta r}, \tag{4.1a}$$

$$f^r = \partial_r\overline{\sigma}^{rr} + \partial_\theta\overline{\sigma}^{\theta r} + \frac{1}{r}\overline{\sigma}^{rr} - r\overline{\sigma}^{\theta\theta}, \tag{4.1b}$$

and, due to symmetry, $f^y = 0$. In the bulk both f^θ and f^r vanish identically. However, f^θ, which proves to be independent of θ outside the interface, if integrated over an elementary volume containing the interface between media 2 and 3, yields the force $dF_\perp = r dF^\theta = r^2 dr dy \int d\theta f^\theta \equiv dF_\perp|_{\theta_0+0} - dF_\perp|_{\theta_0-0}$ acting on every surface element $dr dy$ of the interface [40]. The corresponding normal pressure $P_\perp = dF_\perp/dr dy$ tends either to collapse or unfold the wedge [see Fig. 1(b)]:

$$P_\perp = \frac{8}{r^3}\int_0^\infty d\widetilde{\nu}\nu \frac{\lambda_{+--}\sinh 2\nu(\theta_0 - \pi) - \lambda_{-+-}\sinh 2\nu\theta_0}{W}.$$

This pressure is finite because the divergences on either side of the interface have opposite signs; hence, $P_\perp$ is independent of the cutoff $\nu_{\max}$! First, a few clarifications about the sign of $P_\perp$ follow, which can be illustrated using the asymptotics of the integrand $\mathcal{I}$ in the expression for $P_\perp$:

$$\theta_0 \to 0:\ \mathcal{I} \sim \frac{(\varepsilon_1 - \varepsilon_3)(\varepsilon_3 - \varepsilon_2)}{2(\varepsilon_1 + \varepsilon_2)\varepsilon_3}, \tag{4.2a}$$

$$\theta_0 \to \pi:\ \mathcal{I} \sim \frac{(\varepsilon_1 - \varepsilon_2)(\varepsilon_3 - \varepsilon_2)}{2(\varepsilon_1 + \varepsilon_3)\varepsilon_2}. \tag{4.2b}$$

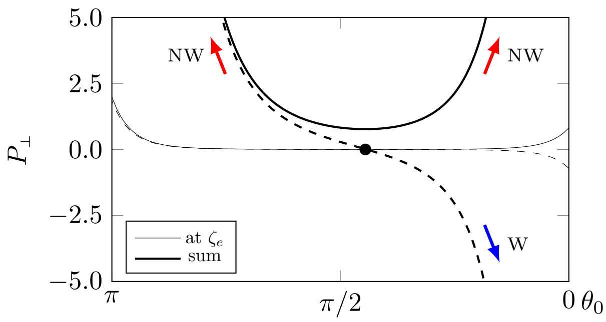

FIG. 3. Plot of $P_\perp$ for water shown at a single absorption frequency $\zeta = \omega_a$ and summed over all Matsubara frequencies ζ_n using the corresponding $\varepsilon(\zeta_n)$ dependence [13]: solid curves correspond to water on mica, and dashed ones to carbon disulfide on Teflon. Red arrows show the nonwetting (NW) tendency to turn away from $\theta_0 = 0$ towards π. The blue arrow shows the wetting (W) tendency $\theta_0 \to 0$.

As we know from the planar-geometry case [7,29,33], the force between two dielectric media ε_1 and ε_2 separated by the vacuum $\varepsilon_3 = 1$ corresponding to the limit (4.2a) is $P_\perp < 0$, implying attraction between the two dielectrics. The other limit (4.2b) can be verified with a liquid-helium film on glass, $\varepsilon_1 > \varepsilon_2$, which leads to $P_\perp < 0$ corresponding to repulsion in this case, consistent with the tendency of the liquid-helium film to thicken [29].

An example computation of $P_\perp$ for a single frequency $\zeta = \omega_a$ and a sum over all Matsubara frequencies using empirical dependence $\varepsilon(\zeta_n)$ is demonstrated in Fig. 3 for (a) water on mica, which is known to wet perfectly, with the macroscopic contact angle being 0°–5°, and (b) carbon disulfide on Teflon, which on a macroscopic scale exhibits the macroscopic contact angle of 80°. Let us first consider the implications of the computed $P_\perp$ in isolation from the surface-tension effects; this is possible since $P_\perp$ does not account for any contributions to interfacial tensions because in the sharp interface formulation considered here, due to antisymmetry of the stresses, the latter provide zero contribution to these tensions [37,39]. In case (a) the fact that $P_\perp$ is positive and nonzero implies that there is no mechanical equilibrium (angle θ_0), i.e., the wedge interface tends to turn to $\theta_0 = \pi$. In case (b) there is an equilibrium angle, but it is obviously unstable, so the contact angle θ_0 may collapse either to zero or π, as dictated by the minimum of potential energy including not only the surface-tension energy but also the energy of the van der Waals stress field. The same behavior as that for water on mica is exhibited for water on PVC, which is known to be nonwetting, and for benzene on fused quartz, which exhibits the macroscopic contact angle of 11°. In the latter case the liquid is nonpolar, and hence, the Lifshitz theory accounting for only London forces should be more accurate, although it is still widely applied even to polar liquids such as water [13]; in the latter case, one can anticipate that due to the polarity of water molecules, which leads to strong hydrogen bonds, and the Keesom effect dominating that of London, the deviations from the Lifshitz theory could be significant [39]. Both generic upward parabola and cotangentlike curves shown in Fig. 3 demonstrate either perfect wetting or nonwetting: even if equilibria exist, they prove to be unstable. The only stable situation would be possible if the cotangentlike curve in Fig. 3 is mirror reflected to become tangentlike. However, as follows from the asymptotics (4.2), for a typical wetting situation when $\varepsilon_2 \approx 1$, this would require $\varepsilon_1 > \varepsilon_3$, thus violating the Lifshitz limit at $\theta_0 \to \pi$. Hence, for all liquid-on-solid wetting situations with air being phase 2, there is no stable contact angle θ_0 other than zero or π, should one focus on the force $P_\perp$ alone. However, if one considers a liquid wedge on a solid substrate, then it is known from classical macroscopic considerations that minimization of the sum of energies of all interfaces leads to the Young equation [41], $\gamma_{21} - \gamma_{31} = \gamma_{23} \sin\theta_0$, which can be viewed as the projection of surface-tension forces (Young's force diagram) on the substrate plane. This equation, however, does not account for the bulk van der Waals stresses, which makes Young's equation inapplicable near the wedge corner in the same way that one would not apply it to solids, where internal stresses play the dominant role. Therefore, as opposed to the commonly used Frumkin-Derjaguin approach [42,43], in which Young's equation stays unmodified in the presence of disjoining pressure, the correct force balance should add the projection of the resultant van der Waals force $-\langle P_\perp\rangle \sin\theta_0$ acting on the interface between media 2 and 3 to Young's equation. Since surface-tension forces applied to flat interfaces in the Young force diagram are independent of the distance r to the wedge tip, at sufficiently short distances they are dominated by $dF_\perp \sim r^{-3}$, which tends to turn the wedge interface toward either $\theta_0 = 0$ or π. When the nonzero width of the interface between media 2 and 3 is taken into account, this happens at distances close to the interface thickness, i.e., on the order of a few molecular distances a_0, where van der Waals stresses and their part contributing to surface tension become inseparable [39]. As a result, our study establishes that the contact angle θ_0 reported in the literature from macroscopic observations is different from the actual one, at which the interface meets the substrate, and instead is set asymptotically at the distances r where surface-tension effects become dominant, thus leading to the classical Young force diagram. Therefore, the wedge interface between media 2 and 3 must necessarily be curved, which also follows from the nonuniformity of pressure $P_\perp$ along the interface.

The presented theory is applicable to the case of a wedge dynamically moving with velocity V along the substrate, i.e., the moving contact-line problem. Clearly, the viscous stresses $\sim\mu V/r$ are on the order of the Derjaguin stresses computed here at $r^* \sim \sqrt{A_\mathrm{H}/6\pi\mu V} \sim 100\,\mathrm{nm}$, where A_H is taken for water on mica. Below this scale, the Derjaguin stresses dominate due to the r^{-3} divergence. Effectively, this means that for $r < r^*$ the liquid cannot be considered Newtonian with the same bulk viscosity μ as that for $r > r^*$. The increased, but nondivergent, stresses for $r < r^*$ enable tearing the "solidified" liquid off the substrate, thus naturally resolving, at the microscopic level, the Huh-Scriven paradox of a singular friction force at the contact line. In the context of the present discussion, it transpires that the paradox arose from the assumption that liquids behave ordinarily regardless of the distance to the contact line.

V. CONCLUSIONS

In this study we were interested in understanding the quantum EM stresses in a static wedge of a dielectric material in the vicinity of its tip and, as a tool, used the Lifshitz theory of van der Waals forces. Since the latter is applicable at distances r greater than interatomic a_0, it was natural to limit the range of our focus from above by the wavelength λ_a of the EM absorption peak, i.e., to $a_0 \lesssim r \lesssim \lambda_a$, which enabled significant simplification of the theory while still serving the main purpose of our work. This range corresponds to the Derjaguin approximation as the effects of retardation are negligible at these scales and all computations can be accurately performed in the nonretarded setting from the very beginning, e.g., by working in the Coulomb gauge $\nabla^i A_i = 0$ and keeping only the terms dependent on A_0. The geometry of the problem inevitably required a local version of the theory, i.e., determining the pointwise distribution of stresses due to spatial anisotropy.

The key findings are as follows. First, the stress distribution is no longer isotropic as it would be in classical fluid mechanics with isotropic pressure on the diagonal of the stress tensor; therefore, the concept of disjoining pressure is replaced by disjoining (or conjoining) stresses. Second, for most common liquid-air-solid triple-point combinations, the contact angle θ_0 either collapses to $\theta_0 = 0$ or unfolds to $\theta_0 = \pi$, which in the case of a liquid wedge corresponds to perfect wetting and nonwetting, respectively. The presented theory reveals the quantum nature of the forces governing the wedge behavior near its tip, being the result of increasingly dominant vacuum polarization. One can say that compared to the fluid in the bulk, where its pressure is isotropic in accordance with Pascal's principle, fluid's behavior near the wedge tip is anomalous due to anisotropy of the stresses in the sense that it becomes akin to solids. This conclusion resurrects Derjaguin's idea, although later denied by Derjaguin himself [44] on the basis of suspected contaminants in experiments, that water in sufficiently small amounts behaves abnormally. As our study shows, even without contaminants, when a liquid's volume is small enough, its properties are strongly affected by the presence of interfaces.

The derivation presented here can be extended to retarded potentials leading to Casimir forces on the dielectric wedge in the same manner as originally done by Lifshitz [7], which is beyond the scope of this work but represents a promising future direction of research. Also, the calculation of finite-temperature corrections might be helpful for more accurate predictions of experimental observations.

ACKNOWLEDGMENTS

This work was partially supported by the Natural Sciences and Engineering Research Council of Canada (NSERC). A.Z. also acknowledges financial support by the Killam Trust.

APPENDIX A: A TIME-DEPENDENT DIPOLE ABOVE A DIELECTRIC HALF-SPACE

Since we were interested in quantum effects at scales shorter than the wavelength λ_a of the electromagnetic absorption peak, our derivation above was based on the nonretarded limit of the Maxwell equations in the Coulomb gauge, which is grounded in the fact that the limit from a complete relativistic Lifshitz theory to its nonretarded case gives asymptotically the same result as that obtained by working out the Lifshitz theory in the nonretarded approximation from the very beginning. As an illustration, here we treat the classical problem of Casimir and Polder [34] of interaction between a time-dependent dipole (such as an anisotropic atom) with a moment $\boldsymbol{p}(t)$, placed in the upper ($z > 0$) dielectric medium characterized by frequency-dependent permittivity $\varepsilon_2(\zeta)$, with the lower half-space of dielectric permittivity $\varepsilon_1(\zeta)$. Computations in the complete retarded theory can be conveniently performed in either the Weyl, $A_0 = 0$ [33], or Lorenz, $\nabla^\nu A_\nu = 0$ [45,46] gauge.

Here we follow Lifshitz and Pitaevskii [33] in the Weyl gauge, in which the Maxwell equations read

$$\nabla_k \nabla^k A_i - \nabla_i \nabla^k A_k - \varepsilon\, \zeta^2 A_i = -\widehat{j}_i, \tag{A1}$$

where the current density $\widehat{j}_i$ of the time-dependent dipole moment $p^k(t)$, written here in Fourier space in terms of the Euclidean time-Fourier transform $\widehat{p}^k(\zeta)$, is

$$\widehat{j}^{t_E}(\zeta) = \widehat{p}^k(\zeta)\partial_k \delta(\boldsymbol{x}, \boldsymbol{x}'), \qquad \widehat{j}_{t_E}(\zeta) = \widehat{j}^{t_E}(\zeta), \tag{A2a}$$

$$\widehat{j}^k(\zeta) = -i\zeta\, \widehat{p}^k(\zeta)\delta(\boldsymbol{x}, \boldsymbol{x}'); \tag{A2b}$$

here $\boldsymbol{x}'$ is the position of the dipole. Our goal is to compute the force acting on such a dipole positioned at the distance z above the interface. Since the problem is conservative, the calculation of this force can be reduced to that of the Casimir-Polder potential U such that $f_i = -\partial_i U$, where it can be shown that in the Weyl gauge this potential naturally depends only on the spatial components of the vector potential A_i:

$$U = \frac{1}{2\beta} \sum_n \widehat{p}^i \widehat{p}^{j'} \zeta_n^2 \Delta \widehat{G}^{\beta}_{ij'}(\zeta_n; \boldsymbol{x}, \boldsymbol{x}')|_{\boldsymbol{x}=\boldsymbol{x}'}, \tag{A3}$$

where $\Delta \widehat{G}^{\beta}_{ij'} = \widehat{G}^{\beta}_{ij'} - \widehat{G}^{\beta(\mathrm{div})}_{ij'}$ and $\widehat{G}^{\beta}_{ij'}$ are the time-Fourier components of the Euclidean Green's function

$$G^{\beta}_{ij'}(t_E - t'_E; \boldsymbol{x}, \boldsymbol{x}') = \langle \mathrm{A}_i(t_E, \boldsymbol{x}) \mathrm{A}_j(t'_E, \boldsymbol{x}) \rangle, \tag{A4}$$

which describes the quantum mean value of the product of operators corresponding to vector potential A_i. In accordance with the Lifshitz subtraction procedure, $\widehat{G}^{\beta(\mathrm{div})}_{ij'}$ is the Green's function of the Maxwell field in a homogeneous dielectric (without interfaces) of permittivity ε.

The Green's function satisfies the equation

$$\left(\delta^j_i \nabla_k \nabla^k - \nabla_i \nabla^j - \varepsilon \zeta^2 \delta^j_i\right) \widehat{G}^{\beta}_{jk'}(\zeta; \boldsymbol{x}, \boldsymbol{x}') = -\delta_{ik'} \delta(\boldsymbol{x}, \boldsymbol{x}').$$

Expanding in Fourier modes in the x and y directions, we get

$$\widehat{G}^{\beta}_{ij'}(\zeta; \boldsymbol{x}, \boldsymbol{x}') = \int \frac{dq_x dq_y}{(2\pi)^2} e^{iq_x(x-x') + iq_y(y-y')} D_{ij'}, \tag{A5}$$

with $D_{ij'} = D_{ij'}(\zeta; q_x, q_y; z, z')$. Without loss of generality we can choose the momentum directed along the x coordinate [33], so that $q_x = q$, $q_y = 0$. Then the set of equations for $D_{ij'}$ in each medium takes the form

$$\left(\partial_z^2 - \varepsilon \zeta^2\right) D_{xx'} - iq \partial_z D_{zx'} = -\delta(z - z'), \tag{A6a}$$

$$\left(\partial_z^2 - w^2\right)D_{yy'} = -\delta(z-z'), \tag{A6b}$$

$$-w^2 D_{zz'} - iq\partial_z D_{xz'} = -\delta(z-z'), \tag{A6c}$$

$$\left(\partial_z^2 - w^2\right)D_{yx'} = 0, \tag{A6d}$$

$$-w^2 D_{zx'} - iq\partial_z D_{xx'} = 0, \tag{A6e}$$

$$\left(\partial_z^2 - \varepsilon\zeta^2\right)D_{xy'} - iq\partial_z D_{zy'} = 0, \tag{A6f}$$

$$-w^2 D_{zy'} - iq\partial_z D_{xy'} = 0, \tag{A6g}$$

$$\left(\partial_z^2 - \varepsilon\zeta^2\right)D_{xz'} - iq\partial_z D_{zz'} = 0, \tag{A6h}$$

$$\left(\partial_z^2 - w^2\right)D_{yz'} = 0, \tag{A6i}$$

where we introduced $w(\zeta,\varepsilon) = \sqrt{q^2 + \varepsilon(\zeta)\zeta^2}$, so that $w_m = w(\zeta, \varepsilon_m)$ for $m = 1, 2$. From Eqs. (A6d) and (A6i) we have $D_{yx'} = 0$, $D_{yz'} = 0$, and using symmetry with respect to interchanging $\boldsymbol{x}$ and $\boldsymbol{x}'$, we also have $D_{xy'} = 0$, $D_{zy'} = 0$. After some algebra we are left with the set of independent equations

$$\left[\partial_z^2 - w^2\right]D_{yy'} = -\delta(z-z'), \tag{A7a}$$

$$\left[\partial_z^2 - w^2\right]D_{xx'} = -\frac{w^2}{\varepsilon\zeta^2}\delta(z-z'), \tag{A7b}$$

$$D_{xz'} = \frac{iq}{w^2}\partial_{z'}D_{xx'}\left(D_{zx'} = -\frac{iq}{w^2}\partial_z D_{xx'}\right), \tag{A7c}$$

$$D_{zz'} = \frac{\delta(z-z')}{w^2} + \frac{q^2}{w^4}\partial_z\partial_{z'}D_{xx'}. \tag{A7d}$$

The boundary conditions for (A7) at $z = 0$ follow from the continuity of the tangential components of the electric and magnetic fields at the interface [33]:

$$[D_{xx'}]_1^2 = [D_{xz'}]_1^2 = [D_{yy'}]_1^2 = 0, \tag{A8a}$$

$$\left[\frac{\varepsilon}{w^2}\partial_z D_{xx'}\right]_1^2 = 0, \tag{A8b}$$

$$[\partial_z D_{yy'}]_1^2 = 0, \tag{A8c}$$

$$[-iqD_{zz'} + \partial_z D_{xz'}]_1^2 = 0, \tag{A8d}$$

where $[\cdot]_1^2$ stands for the jump in values across the interface between media 1 and 2. As soon as we compute $D_{xx'}$ and $D_{yy'}$, the nondiagonal components $D_{xz'}$ and $D_{zx'}$ can be found from (A7c). To calculate $D_{yy'}(\zeta, q_x, q_y; z, z')$ we look for the solution in the form

$$D_{yy'} = \frac{1}{2\,w_2}\begin{cases} a\,e^{-w_2 z} + e^{-w_2|z-z'|}, & z > 0,\\ b\,e^{w_1 z}, & z < 0,\end{cases} \tag{A9}$$

where the constants are fixed by the corresponding boundary conditions (A8a) and (A8c) and prove to be

$$a = r_{\rm TE}e^{-w_2 z'}, \qquad b = \frac{2\,w_2}{w_2 + w_1}e^{-w_2 z'}. \tag{A10}$$

Here we introduced the conventional notation for the transverse electric Fresnel coefficient $r_{\rm TE} = (w_2 - w_1)/(w_2 + w_1)$ [45], and for later purposes we will also need the transverse magnetic Fresnel coefficient $r_{\rm TM} = (\varepsilon_1 w_2 - \varepsilon_2 w_1)(\varepsilon_1 w_2 + \varepsilon_2 w_1)$; both are functions of the imaginary frequency ζ. Since we are interested in finding the force acting on the dipole located in the upper half-space $z > 0$ and because the current density (A2a) is concentrated at $z' > 0$, the relevant part leading to the divergent Green's function, which describes the solution in the homogeneous space without interfaces, is

$$D_{yy'}^{(\rm div)} = \frac{1}{2w_2}e^{-w_2|z-z'|}, \tag{A11}$$

while the other part, which accounts for finite observable effects, has the form

$$\Delta D_{yy'} = D_{yy'} - D_{yy'}^{(\rm div)} = \frac{r_{\rm TE}}{2\,w_2}e^{-\nu_2(z+z')}. \tag{A12}$$

The corresponding Green's functions in the coordinate space

$$G_{yy'}^{\beta(\rm div)}(\zeta;\boldsymbol{x},\boldsymbol{x}') = \frac{1}{2\pi}\int_0^\infty dq\,q\,J_0(qr)\frac{e^{-w_2|z-z'|}}{2w_2}$$
$$= \frac{1}{4\pi}\frac{e^{-\varepsilon_2\zeta^2\sqrt{r^2+(z-z')^2}}}{\sqrt{r^2+(z-z')^2}}, \tag{A13}$$

where $r^2 = (x-x')^2 + (y-y')^2$, and

$$\Delta G_{yy'}^{\beta}(\zeta;\boldsymbol{x},\boldsymbol{x}') = \frac{1}{4\pi}\int_0^\infty dqq\,J_0(qr)\frac{r_{\rm TE}}{w_2}e^{-w_2(z+z')}.$$

The quantity r used here should not be confused with the coordinate r in the cylindrical coordinate system employed in the main text. Other components of the Green's functions are found in a similar fashion. In the computation of the Casimir-Polder potential U we need to know the Green's functions only at the coincident points $\Delta G_{ij} \equiv \Delta G_{ij'}(\zeta;\boldsymbol{x},\boldsymbol{x}')|_{\boldsymbol{x}=\boldsymbol{x}'}$:

$$\Delta G_{yy}^{\beta} = \frac{1}{4\pi}\int_0^\infty dqq\,\frac{r_{\rm TE}}{w_2}e^{-2w_2 z}, \tag{A14}$$

$$\Delta G_{xx}^{\beta} = -\frac{1}{4\pi}\int_0^\infty dqq\,\frac{w_2\,r_{\rm TM}}{\varepsilon_2\zeta^2}e^{-2w_2 z}, \tag{A15}$$

$$\Delta G_{zz}^{\beta} = -\frac{1}{4\pi}\int_0^\infty dqq\,\frac{q^2\,r_{\rm TM}}{w_2\varepsilon_2\zeta^2}e^{-2w_2 z}. \tag{A16}$$

In the cylindrical coordinates (z, r, ϕ) with the z axis going through the dipole position, the fluctuating dipole moment has the components $\widehat{\boldsymbol{p}} = (\widehat{p}^z, \widehat{p}^r, 0)$, with $(\widehat{p}^r)^2 = (\widehat{p}^x)^2 + (\widehat{p}^y)^2$, so that

$$U = \sum_n \frac{\zeta_n^2}{2\beta}\left[(\widehat{p}^z)^2\Delta G_{zz}^{\beta} + \frac{(\widehat{p}^r)^2}{2}\left(\Delta G_{xx}^{\beta} + \Delta G_{yy}^{\beta}\right)\right]. \tag{A17}$$

The factor of $\frac{1}{2}$ in the last term appears due to integration of $\sin^2\phi$ and $\cos^2\phi$ over ϕ in momentum space. Note that the contribution by off-diagonal terms ΔG_{xz}^{β} and ΔG_{zx}^{β} drops out from the expression because of their symmetry with respect to interchanging $\boldsymbol{x}$ and $\boldsymbol{x}'$ [33]. Thermal fluctuation effects at $T = 300$ K are negligible compared to those due to quantum fluctuations at scales that are much shorter than the thermal scale $\hbar c/(k_B T) \sim 7.6\,\mu$m $\gg \lambda_a$. Therefore, at scales below λ_a the sum over the Matsubara frequencies ζ_n can be replaced by the integral [33]

$$\frac{1}{2\beta}\sum_n f(\zeta_n) \to \int_0^\infty \frac{d\zeta}{2\pi}f(\zeta). \tag{A18}$$

Eventually, from (A17) we obtain

$$U = -\int_0^\infty \frac{d\zeta}{2\pi}\int_0^\infty dqq\,\frac{e^{-2w_2 z}}{4\pi\varepsilon_2 w_2}\Big[q^2\, r_{\rm TM}\,(\widehat{p}^z)^2 + \frac{1}{2}\big(w_2^2\, r_{\rm TM} - \varepsilon_2\zeta^2 r_{\rm TE}\big)(\widehat{p}^r)^2\Big], \quad (A19)$$

which for the dipole in the vacuum $\varepsilon_2 = 1$ reproduces the result by Marachevsky [45,46] derived in the Lorentz gauge.

Now let us compare the small-scale $z < \lambda_a$ (nonretarded, i.e., Derjaguin) and large-scale $z > \lambda_a$ (retarded, i.e., Casimir) limits. For simplicity, we restrict our further consideration to $\varepsilon_2 = 1$, in which case $w_2 = \sqrt{q^2+\zeta^2}$. By introducing a dimensionless integration variable $b = w_2/\zeta$, the Casimir-Polder potential can be rewritten in the form

$$U = -\frac{1}{4\pi}\int_1^\infty db\int_0^\infty \frac{d\zeta}{2\pi}\zeta^3\, e^{-2\zeta z b} \times\Big[(b^2-1)\, r_{\rm TM}\,(\widehat{p}^z)^2 + \frac{1}{2}(b^2 r_{\rm TM} - r_{\rm TE})(\widehat{p}^r)^2\Big], \quad (A20)$$

and the Fresnel coefficients become

$$r_{\rm TE} = \frac{b-\sqrt{b^2+\varepsilon_1-1}}{b+\sqrt{b^2+\varepsilon_1-1}},\quad r_{\rm TM} = \frac{\varepsilon_1 b-\sqrt{b^2+\varepsilon_1-1}}{\varepsilon_1 b+\sqrt{b^2+\varepsilon_1-1}}.$$

While one can substitute here a function $\varepsilon_1(\zeta)$ known from experiments [13] and integrate over ζ as we did in Sec. IV, for the purpose of distinguishing between retarded and nonretarded effects we consider a steplike model,

$$\varepsilon_1 = 1 + (\varepsilon - 1)\,\theta(\omega_a - \zeta), \quad (A21)$$

which allows us to perform all integrations analytically and captures all the essential features of the problem we are interested in. The analysis can also be simplified by assuming that the quantum mean value of the dipole moments $\alpha^{ij} = \langle \widehat{p}^i(\zeta)\,\widehat{p}^j(\zeta)\rangle$ does not depend on frequency. Then we get

$$U = U_z\alpha^{zz} + U_r\alpha^{rr},\ \ \alpha^{rr} = \alpha^{xx} + \alpha^{yy}, \quad (A22)$$

where

$$U_z = -\frac{1}{8\pi^2}\int_1^\infty db\, W_z,\ \ U_r = -\frac{1}{8\pi^2}\int_1^\infty db\, W_r, \quad (A23)$$

and the integrands are

$$W_z = \int_0^\infty d\zeta\,\zeta^3\, e^{-2\zeta z b}(b^2-1)\, r_{\rm TM}, \quad (A24a)$$

$$W_r = \int_0^\infty d\zeta\,\zeta^3\, e^{-2\zeta z b}\frac{1}{2}(r_{\rm TM} b^2 - r_{\rm TE}). \quad (A24b)$$

1. Derjaguin's limit: Small distances $\omega_a z \ll 1$

Expanding W_z and W_r for small $\omega_a z$, we obtain

$$W_z = 2\, W_r = \frac{\varepsilon-1}{\varepsilon+1}\frac{1}{8\, b^2 z^4}\{3 - [3 + 6(\omega_a z b) + 6(\omega_a z b)^2 + 4(\omega_a z b)^3]e^{-2\omega_a z b}\} + O(\omega_a z). \quad (A25)$$

Then after integrating (A23), the potentials to leading order become

$$U_z = 2\, U_r \approx -\frac{\varepsilon-1}{\varepsilon+1}\frac{\omega_a}{32\,\pi^2 z^3} + O(z^{-2}), \quad (A26)$$

and

$$U = -\frac{\omega_a}{64\,\pi^2}\frac{\varepsilon-1}{\varepsilon+1}\frac{1}{z^3}[2\,\alpha^{zz} + \alpha^{rr}]. \quad (A27)$$

Note that the contribution of only zero-frequency mode ζ_0 can be found directly from (A14)–(A17),

$$U^{(0)} = -\frac{1}{64\pi\,\beta}\frac{\varepsilon-1}{\varepsilon+1}\frac{1}{z^3}[2\alpha^{zz} + \alpha^{rr}]. \quad (A28)$$

A comparison of $U^{(0)}$ and U, i.e., (A28) and (A27), in the Derjaguin limit shows that, as expected, $U = NU^{(0)}$, where $N = \beta\,\omega_a/\pi$ is the number of Matsubara modes in the interval $-\omega_a \leqslant \zeta_n \leqslant \omega_a$. Thus, for the model (A21) only Matsubara modes $|\zeta_n| \leqslant \omega_a$ contribute (equally) to the force. In the general case of a realistic $\varepsilon_1(\zeta)$, each mode would contribute with the weight $\frac{\varepsilon_1(\zeta)-1}{\varepsilon_1(\zeta)+1}[2\,\alpha^{zz}(\zeta) + \alpha^{rr}(\zeta)]$. Because at large frequencies $\varepsilon_1 \to 1$, the integrals (A24) converge. Higher-order corrections to the Derjaguin limit of the Casimir-Polder potential U are due to the retardation effects and are smaller than the main contribution (A27) by a factor of $(\omega_a z)^3/3 \ll 1$. It is straightforward to demonstrate that the result (A27) obtained by taking the nonretarded limit of the complete relativistic Lifshitz theory is exactly the same as that deduced by solving the problem in the nonretarded setting from the very beginning, e.g., in the Coulomb gauge (see Sec. A 3).

2. Casimir's limit: Large distances $\omega_a z \gg 1$

In this limit the contribution of large frequencies is exponentially suppressed, and (A24a) leads to

$$W_z = \frac{3}{8}\frac{(b^2-1)}{b^4}\frac{r_{\rm TM}}{z^4} + O(e^{-2\omega_a b z}), \quad (A29a)$$

$$W_r = \frac{3}{16}\frac{1}{b^4}\frac{1}{z^4}[b^2 r_{\rm TM} - r_{\rm TE}] + O(e^{-2\omega_a b z}). \quad (A29b)$$

Integrals over the parameter b give (A22), where

$$U_z = -\frac{1}{32\pi^2 z^4}C_z(\varepsilon),\ \ U_r = -\frac{1}{32\pi^2 z^4}C_r(\varepsilon), \quad (A30)$$

with $C_z(\varepsilon)$ and $C_r(\varepsilon)$ computable analytically. For large $\varepsilon \gg 1$ their asymptotics are $C_z = 1 + O(\varepsilon^{-1/2})$ and $C_r = 1 + O(\varepsilon^{-1/2})$, so that

$$U = -\frac{1}{32\pi^2 z^4}[\alpha^{zz} + \alpha^{rr}]. \quad (A31)$$

This result reproduces the Casimir-Polder potential for a dipole above the metal [34]. At large scales the dependence on the absorption frequency drops out, as it should in the Casimir effect.

3. A dipole above a half-space in the nonretarded setting

At small distances the physics is governed by the Derjaguin limit, which using the Coulomb gauge can be reduced to the computation of only one Green's function G_{00}. After the Wick rotation it can be written as the Fourier time series (2.3), where for each Matsubara frequency $\zeta = \zeta_n$ we have

$$\nabla_i[\varepsilon(\zeta)\nabla^i]\widehat{G}^\beta(\zeta;\boldsymbol{x},\boldsymbol{x}') = \delta(\boldsymbol{x},\boldsymbol{x}'), \tag{A32}$$

with $\boldsymbol{x} = (x, y, z)$. At the interface between two dielectrics with ε_1 and ε_2, the Green's function $\widehat{G}^\beta$ must satisfy the boundary conditions (2.5).

After the Fourier decomposition in the x and y directions

$$\widehat{G}^\beta(\zeta;\boldsymbol{x},\boldsymbol{x}') = \int \frac{dq_x dq_y}{(2\pi)^2} e^{iq_x(x-x')+iq_y(y-y')} D, \tag{A33}$$

the Fourier-transformed Green's function $D = D(\zeta; q_x, q_y; z, z')$ inherits the following equation and boundary conditions:

$$\left(\partial^2_{zz} - q^2\right)D = \frac{1}{\varepsilon}\delta(z - z'), \quad q = \sqrt{q_x^2 + q_y^2}, \tag{A34a}$$

$$D_1 = D_2, \quad \varepsilon_1\partial_z D|_1 = \varepsilon_2\partial_z D|_2. \tag{A34b}$$

Consider the point $\boldsymbol{x}'$ inside the slab of the dielectric with ε_2. First, we look for a solution of (A34a) which vanishes for $z \to \pm\infty$:

$$D = \begin{cases} a\, e^{-qz} - \frac{1}{2q\varepsilon_2} e^{-q|z-z'|}, & z > 0, \\ b\, e^{qz}, & z < 0. \end{cases} \tag{A35}$$

Next, using the boundary conditions (A34b) at $z = 0$, we find the coefficients a and b,

$$a = \frac{1}{2q\varepsilon_2}\frac{\varepsilon_1 - \varepsilon_2}{\varepsilon_1 + \varepsilon_2} e^{-qz'}, \quad b = -\frac{1}{q}\frac{1}{\varepsilon_1 + \varepsilon_2} e^{-qz'}. \tag{A36}$$

In the absence of the interface, the corresponding Green's function would be

$$D^{(\mathrm{div})} = -\frac{1}{2q\varepsilon_2} e^{-q|z-z'|}. \tag{A37}$$

Thus, in the sector $z, z' > 0$ we have $D = D^{(\mathrm{div})} + \Delta D$, where ΔD is the contribution left after the Lifshitz subtraction:

$$\Delta D = \frac{1}{2q\varepsilon_2}\frac{\varepsilon_1 - \varepsilon_2}{\varepsilon_1 + \varepsilon_2} e^{-q(z+z')}. \tag{A38}$$

Upon the inverse Fourier transform of ΔD back to the coordinate space we get

$$\Delta G(\zeta;\boldsymbol{x},\boldsymbol{x}') = \frac{1}{4\pi\varepsilon_2}\frac{\varepsilon_1 - \varepsilon_2}{\varepsilon_1 + \varepsilon_2}\frac{1}{\sqrt{r^2 + (z + z')^2}}. \tag{A39}$$

In accordance with the Lifshitz subtraction, we consider the difference ΔA_{t_E} of the vector potential A_{t_E} and the "vacuum" one $A^{(\mathrm{div})}_{t_E}$ in the homogeneous media with ε_2:

$$\Delta A_{t_E}(\zeta;\boldsymbol{x},\boldsymbol{x}') = \int d\boldsymbol{x}''\Delta G(\zeta;\boldsymbol{x},\boldsymbol{x}'') j_{t''_E}(\zeta;\boldsymbol{x}'',\boldsymbol{x}'),$$

where $j_{t_E}(\zeta,\boldsymbol{x},\boldsymbol{x}')$ is given by (A2a). We assume that the pointlike dipole is located at $\boldsymbol{x}' = (0, 0, z')$; then

$$\Delta A_{t_E}(\zeta;\boldsymbol{x},\boldsymbol{x}') = -[\widehat{p}^k\partial_{x'^k}]\Delta G(\zeta;\boldsymbol{x},\boldsymbol{x}'), \tag{A40}$$

and the corresponding contribution to the Maxwell field reads

$$\Delta F_{it_E} = \partial_i(\Delta A_{t_E}).$$

The force density f_i acting on the dipole p^k in turn takes the form

$$f_i = \Delta F_{it_E} j^{t_E} = \tfrac{1}{2}\partial_i([\widehat{p}^m\partial_m][\widehat{p}^{k'}\partial_{k'}]\Delta G(\zeta;\boldsymbol{x},\boldsymbol{x}')\big|_{x=x'}),$$

and only the z component of the force $f_i = (0, 0, f_z)$ is nonvanishing,

$$f_z(\zeta) = -\frac{3}{64\pi\varepsilon_2}\frac{\varepsilon_1(\zeta) - \varepsilon_2(\zeta)}{\varepsilon_1(\zeta) + \varepsilon_2(\zeta)}[2\alpha^{zz} + \alpha^{rr}]\frac{\delta(\boldsymbol{x},\boldsymbol{x}')}{z'^4}.$$

The force acting on the dipole is the integral over the space and the sum over all Matsubara frequencies

$$\mathcal{F}_z = \frac{1}{\beta}\sum_n \int d\boldsymbol{x} f_z(\zeta_n). \tag{A41}$$

At small distances from the interface the temperature effects are negligible, and the sum in (A41) can be replaced by the integral

$$\mathcal{F}_z = 2\int_0^\infty \frac{\mathrm{d}\zeta}{2\pi}\int d\boldsymbol{x} f_z(\zeta). \tag{A42}$$

For the toy model (A21) of steplike ε_1 and $\varepsilon_2 = 1$ the final result for the force in the Derjaguin limit becomes

$$\mathcal{F}_z = -\partial_z U, \tag{A43}$$

$$U = -\frac{\omega_a}{64\pi^2}\frac{\varepsilon - 1}{\varepsilon + 1}\frac{1}{z^3}[2\alpha^{zz} + \alpha^{rr}], \tag{A44}$$

which exactly reproduces the small $\omega_a z$ limit (A27) of the force derived using the complete retarded calculations. This confirms the expectation that, at small scales in comparison to the absorption wavelength, one may neglect all retardation effects and perform much simpler (nonretarded) calculations instead.

APPENDIX B: BASIC FORMULAS IN CYLINDRICAL COORDINATES

The EM stress-energy tensor in an arbitrary coordinate system has the form

$$T^{\mu\nu} = F^{\mu\alpha}D^\nu{}_\alpha - \tfrac{1}{4}g^{\mu\nu}F_{\alpha\beta}D^{\alpha\beta}, \tag{B1}$$

where $\mu, \nu = (0, 1, 2, 3)$. The spatial components of this tensor give the stress tensor with the standard sign convention [24]

$$\sigma^{ij} = -T^{ij}, \quad i, j = (1, 2, 3). \tag{B2}$$

At small scales $\lesssim \lambda_a$, where the nonretarded approximation produces the leading contribution, one can use the Coulomb gauge $\nabla_i A^i \equiv A^i{}_{;i} = 0$ and keep only the terms involving A_0. In the standard notations a semicolon denotes the covariant derivative defined using the metric g_{ij}, while a comma denotes the partial derivative. Therefore, the only component of the Maxwell tensor that contributes in the nonretarded limit is $F_{0i} = -\nabla_i A_0 \equiv -A_{0;i}$ and $D_{0i} = \varepsilon F_{0i}$. Substituting these into (B2), we obtain (3.1) for the stress tensor of the Maxwell field in the nonretarded limit. Note that in the Minkowski signature $F_{0i}F^0{}_j = -A_{0;i}A_{0;j}$, while in the Euclidean one we have

$F_{t_E i}F^{t_E}{}_j = A_{t_E;i}A_{t_E;j}$. Substituting these relations into (B2) and (B3), we obtain (3.1).

Raising and lowering spatial indices are performed using the metric g_{ij}. For example, in the cylindrical coordinates $x^i = (r, \theta, y)$ we have $g_{ij} = \mathrm{diag}(1, r^2, 1)$ and $g^{ij} = \mathrm{diag}(1, r^{-2}, 1)$. Then for the renormalized Fourier components of the stress tensor we get $\overline{\sigma}_{ij} = g_{ik}g_{jl}\overline{\sigma}^{kl}$, or explicitly,

$$\overline{\sigma}_{rr} = \overline{\sigma}^{rr},\ \overline{\sigma}_{\theta\theta} = r^4\overline{\sigma}^{\theta\theta},\ \overline{\sigma}_{r\theta} = r^2\overline{\sigma}^{r\theta},\ \overline{\sigma}_{yy} = \overline{\sigma}^{yy}.$$

The force density reads

$$f^i = \overline{\sigma}^{ik}{}_{;k} = \overline{\sigma}^{ik}{}_{,k} + \Gamma^i_{jk}\overline{\sigma}^{jk} + \Gamma^k_{jk}\overline{\sigma}^{ij}. \tag{B3}$$

The necessary nonvanishing components of the Christoffel symbols Γ^i_{jk} are

$$\Gamma^r_{\theta\theta} = -r,\ \ \Gamma^\theta_{r\theta} = \frac{1}{r},\ \ \Gamma^k_{rk} = \frac{1}{r}. \tag{B4}$$

Substitution of these expressions into (B3) leads to the components of the force density (4.1).

---

[1] In general, van der Waals forces include effects of orientation [47], induction [48], and both nonretarded [49] and retarded [34] dispersion intermolecular potentials.

[2] J. D. van der Waals, Over de continuiteit van den gas-en vloeistoftoestand, Ph.D. thesis, Leiden University, 1873.

[3] B. Derjaguin, Untersuchungen über die Reibung und Adhäsion, IV, Kolloid Z. **69**, 155 (1934); B. V. Derjaguin and M. M. Kusakov, The properties of thin layers of liquids, Proc. Acad. Sci. USSR, Chem. Ser. **5**, 741 (1936); H. C. Hamaker, The London – van der Waals attraction between spherical particles, Physica (Amsterdam) **4**, 1058 (1937).

[4] The Hamaker constant reflects the strength of the molecular interaction between specific macroscopic bodies.

[5] Functional dependence ℓ^{-3} is still the same, however.

[6] B. V. Derjaguin, A. S. Titijevskaia, I. I. Abricossova, and A. D. Malkina, Investigations of the forces of interaction of surfaces in different media and their application to the problem of colloid stability, Discuss. Faraday Soc. **18**, 24 (1954); B. V. Deryaguin, I. I. Abrikosova, and E. M. Lifshitz, Direct measurement of molecular attraction between solids separated by a narrow gap, Q. Rev., Chem. Soc. **10**, 295 (1956). B. V. Deryaguin, The force between molecules, Sci. Am. **203**, 47 (1960); D. Tabor and R. H. S. Winterton, Direct measurement of normal and retarded van der Waals forces, Nature (London) **219**, 1120 (1968).

[7] E. M. Lifshitz, The theory of molecular attractive forces between solids, Sov. Phys. JETP **2**, 73 (1956).

[8] Dispersion forces are called so due to the molecules polarizability, which in turn is related to the refractive index and thus dispersion.

[9] Unless rarefied, polarizability of condensed matter may be vastly different from that of an individual molecule.

[10] C. Farina, F. C. Santos, and A. C. Tort, A simple way of understanding the nonadditivity of van der Waals dispersion forces, Am. J. Phys. **67**, 344 (1999).

[11] This fact is based on the Kramers-Kroning relation [33]: their imaginary parts are always positive and determine the energy dissipation of the EM wave propagating in the medium.

[12] S. M. Rytov, *Theory of Electrical Fluctuations and Thermal Radiation* (USSR Academy of Sciences Publishing House, Moscow, 1953).

[13] J. Israelachvili, *Intermolecular and Surface Forces* (Academic Press, San Diego, 2011).

[14] A simple calculation of the intermolecular potential for a wedge [50] brought some ideas about the forces driving wetting. Assuming that the intermolecular potential Φ is constant along the interface of the wedge with the contact angle θ_0 at equilibrium, this led [51] to the disjoining pressure in the small-slope $\ell_x \ll 1$ limit $\Pi_{\mathrm{D}}(\ell, \ell_x) \sim -(\theta_0^4 - \ell_x^4)/\ell^3$, which is potentially regular at $\ell \to 0$. Requiring further that Φ is constant (minimized) not only at the interface but also inside the wedge [52] produced $\Pi_{\mathrm{D}}(\ell, \ell_x, \ell_{xx}) \sim -(\theta_0^4 - \ell_x^4 + 2\ell\ell_x^2\ell_{xx})/\ell^3$, which, however, does not recover the planar film formula; a fix for this issue was recently [53] suggested.

[15] M. V. Berry, The molecular mechanism of surface tension, Phys. Educ. **6**, 79 (1971).

[16] A. I. Rusanov and A. K. Shchekin, Local mechanical equilibrium conditions for interfaces and thin films of arbitrary shape, Mol. Phys. **103**, 2911 (2005); On the definition of the disjoining pressure of a wedge-shaped film, **105**, 3185 (2007).

[17] J. Schwinger, L. L. Deraad, Jr., and K. A. Milton, Casimir effect in dielectrics, Ann. Phys. (NY) **115**, 1 (1978).

[18] I. Brevik and M. Lygren, Casimir effect for a perfectly conducting wedge, Ann. Phys. (NY) **251**, 157 (1996).

[19] I. Brevik, M. Lygren, and V. N. Marachevsky, Casimir-Polder effect for a perfectly conducting wedge, Ann. Phys. (NY) **267**, 134 (1998).

[20] I. H. Brevik and K. Pettersen, Casimir effect for a dielectric wedge, Ann. Phys. (NY) **291**, 267 (2001).

[21] I. Brevik, S. Å. Ellingsen, and K. A. Milton, Electrodynamic Casimir effect in a medium-filled wedge, Phys. Rev. E **79**, 041120 (2009).

[22] S. A. Ellingsen, I. Brevik, and K. A. Milton, Electrodynamic Casimir effect in a medium-filled wedge II, Phys. Rev. E **80**, 021125 (2009).

[23] C. W. Misner, K. S. Thorne, and J. A. Wheeler, *Gravitation* (Freeman, San Francisco, 1973).

[24] L. D. Landau and E. M. Lifshitz, *Theory of Elasticity*, Course of Theoretical Physics Vol. 7 (Butterworth-Heinemann, New York, 1986).

[25] Y. S. Barash and V. L. Ginzburg, Electromagnetic fluctuations in matter and molecular (Van-der-Waals) forces between them, Sov. Phys. Usp. **18**, 305 (1975).

[26] L. D. Landau, L. P. Pitaevskii, and E. M. Lifshitz, *Electrodynamics of Continuous Media* (Butterworth-Heinemann, 1984).

[27] Kontorovich-Lebedev transform commonly arises in diffraction problems on wedge-shaped domains.

[28] M. I. Kontorovich and N. N. Lebedev, A method for the solution of problems in diffraction theory and related topics, Zh. Eksp. Teor. Fiz. **8**, 1192 (1938); N. N. Lebedev, Sur une formule d'inversion, Dokl. Akad. Sci. USSR **52**, 655 (1946).

[29] I. E. Dzyaloshinskii, E. M. Lifshitz, and L. P. Pitaevskii, General theory of van der Waals' forces, Sov. Phys. Usp. **4**, 153 (1961).

[30] Physically, this renormalization follows from the chemical potential, which must be constant for media in equilibrium. One may think of the electrostriction stress as being analogous to the gravity in the ocean compensated by the mechanical stresses in water: in a wedge, if it is balanced in the r direction, then due to isotropy it must be balanced in the θ direction as well. Notably, the θ dependence of the electrostriction stress leads to nonuniform compression of the matter which is stronger near the interface [39]. However, due to its isotropy, electrostriction does not contribute to surface tension. The latter originates from anisotropy of the EM (van der Waals) stresses $\overline{\sigma}^{\theta\theta}$ and $\overline{\sigma}^{rr}$ (3.3) near the interface [39].

[31] Isotropy of the mechanical stresses in liquids follows from the short-range nature of the repulsive forces (the r^{-12} term in the Lennard-Jones potential) compared to the long-range van der Waals forces (the r^{-6} term in Derjaguin's approximation), which are responsible for the anisotropy of the stresses near planar interfaces and near the tip of a wedge considered here.

[32] Among them are the Navier-Stokes equations, in which velocity is a contravariant vector; in fact, for direct use in the Navier-Stokes equations the stress-tensor components (3.3) need to be transformed to the physical components.

[33] E. M. Lifshitz and L. P. Pitaevskii, *Statistical Physics, Part 2: Theory of the Condensed State* (Pergamon, New York, 1980).

[34] H. B. G. Casimir and D. Polder, The influence of retardation on the London-van der Waals forces, Phys. Rev. **73**, 360 (1948).

[35] D. Deutsch and P. Candelas, Boundary effects in quantum field theory, Phys. Rev. D **20**, 3063 (1979).

[36] L. S. Brown and G. J. Maclay, Vacuum stress between conducting plates: An image solution, Phys. Rev. **184**, 1272 (1969).

[37] P. Candelas, Vacuum energy in the presence of dielectric and conducting surfaces, Ann. Phys. (NY) **143**, 241 (1982).

[38] M. Bordag, D. Hennigt, and D. Robaschik, Vacuum energy in quantum field theory with external potentials concentrated on planes, 1. Phys. A (Amsterdam, Neth.) **25**, 4483 (1992).

[39] A. Zelnikov and R. Krechetnikov, Scarf for Lifshitz, Eur. Phys. J. Plus **136**, 755 (2021).

[40] The force is expressed here in an invariant form, $dF_\perp = \sqrt{dF_\theta dF^\theta}$, where $dF_\theta = r^2 dF^\theta$.

[41] T. Young, An essay on the cohesion of fluids, Philos. Trans. R. Soc. London **95**, 65 (1805).

[42] A. N. Frumkin, Phenomena of wetting and adhesion of bubbles, Zh. Fiz. Khim. **12**, 337 (1938).

[43] B. V. Derjaguin, Theory of the capillary condensation and other capillary phenomena taking into account the disjoining effect of long-chain molecular liquid films, Zh. Fiz. Khim. **14**, 137 (1940).

[44] B. V. Derjaguin and N. V. Churaev, Nature of "anomalous water," Nature (London) **244**, 430 (1973).

[45] V. N. Marachevsky and A. A. Sidelnikov, Green functions scattering in the Casimir effect, Universe **7**, 195 (2021).

[46] V. N. Marachevsky, The Casimir effect: Medium and geometry, J. Phys. A **45**, 374021 (2012).

[47] W. H. Keesom, The second virial coefficient for rigid spherical molecules whose mutual attraction is equivalent to that of a quadruplet placed at its center, Proc. R. Neth. Acad. Arts Sci. **18**, 636 (1915).

[48] P. Debye, Die van der Waals'schen Kohäsionskräfte, Phys. Z. **21**, 178 (1920).

[49] F. London, Zur Theorie und Systematik der Molecularkrafte, Z. Phys. **63**, 245 (1930); H. B. G. Casimir, On the attraction between two perfectly conducting plates, Proc. K. Ned. Akad. Wet. **51**, 793 (1948).

[50] C. A. Miller and E. Ruckenstein, The origin of flow during wetting of solids, J. Colloid Interface Sci. **48**, 368 (1974).

[51] L. M. Hocking, The influence of intermolecular forces on thin fluid layers, Phys. Fluids **5**, 793 (1993).

[52] Q. Wu and H. Wong, A slope-dependent disjoining pressure for non-zero contact angles, J. Fluid Mech. **506**, 157 (2004).

[53] B. Dai, L. G. Leal, and A. Redondo, Disjoining pressure for nonuniform thin films, Phys. Rev. E **78**, 061602 (2008).